The Ubiquitin−Proteasome Pathway Plays an Essential Role in Proteolysis during *Trypanosoma cruzi* Remodeling†

Juana L. de Diego,*,# Jeffrey M. Katz,# Patricia Marshall,# Bessy Gutiérrez,# Jerry E. Manning,§ Victor Nussenzweig,# and Jorge González‡

Michael Heidelberger Division, Pathology Department, New York University School of Medicine, New York, New York 10016, Department of Molecular Biology and Biochemistry, University of California, Irvine, California 92696-3900, and Parasitology Unit, Health Sciences Faculty, University of Antofagasta, Antofagasta, Chile

Received July 17, 2000; Revised Manuscript Received October 26, 2000

ABSTRACT: Here, we document for the first time the presence of the 26S proteasome and the ubiquitin pathway in a protozoan parasite that is in an early branch in the eukaryotic lineage. The 26S proteasome of *Trypanosoma cruzi* epimastigotes was identified as a high molecular weight complex (1400 kDa) with an ATP-dependent chymotrypsin-like activity against the substrate Suc-LLVY-Amc. This activity was inhibited by proteasome inhibitors and showed same electrophorectic migration pattern as yeast 26S proteasome in nondenaturating gels. About 30 proteins in a range of 25−110 kDa were detected in the purified *T. cruzi* 26S proteasome. Antibodies raised against the AAA family of ATPases from eukaryotic 26S proteasome and the *T. cruzi* 20S core specifically recognized components of *T. cruzi* 26S. To confirm the biological role of 26S in this primitive eukaryotic parasite, we analyzed the participation of the ubiquitin (Ub)−proteasome system in protein degradation during the time of parasite remodeling. Protein turnover in trypomastigotes was proteasome and ATP-dependent and was enhanced during the transformation of the parasites into amastigotes. If 20S proteasome activity is inhibited, ubiquitinated proteins accumulate in the parasites. As expected from the profound morphological changes that occur during transformation, cytoskeletal proteins associated with the flagellum are targets of the ubiquitin−proteasome pathway.

Trypanosoma cruzi, causative agent of Chagas' disease, undergoes profound morphological changes during development in the vertebrate and invertebrate hosts. The trypomastigotes invade the vertebrate host cells and immediately come into contact with the lysosomal compartment (*1*). Most likely, the acidic pH of lysosomes induces the transformation into amastigotes (*2*−*4*). The amastigotes replicate intracellularly and, within several days, transform back into trypomastigotes. During this precisely timed cycle, *T. cruzi* undergoes shape changes, the flagellum and kinetoplast must be remodeled, genes must be turned off and new genes turned on, and proteins must be selectively degraded and synthesized.

In eukaryotic cells, the turnover of intracellular proteins is mediated mainly by the ubiquitin−proteasome system (*5*). Following ubiquitination, proteins are unfolded and degraded by the 26S proteasome, a large multisubunit complex located in the cytosolic and nuclear compartments. This proteolytic pathway controls a broad array of cellular functions, including cell cycle progression (*6*), stage-specific gene transcription (*7*), antigen-processing (*8*), regulation of membrane-anchored and secretory pathway-compartmentalized proteins (*9*), and protein quality control (*10*).

The 26S proteasome is made up of two 19S regulatory complexes and a proteolytically active 20S proteasome core (*11, 12*), which is a cylindrical structure composed of four stacked heptameric rings composed of α-subunits in the outer rings and *β*-subunits in the inner ones (*13*). The active sites reside within the *β*-subunits, which provide the catalytic N-terminal threonine residues (*14*). The substrate is believed to enter through narrow pores in the α-rings, which associate with the regulatory 19S complex in an ATP-dependent manner to form the 26S proteasome. This complex degrades ubiquitin (Ub)-conjugated proteins through a process that also requires the hydrolysis of ATP (*11*). The 19S regulator (*17*) can be further dissociated into two subcomplexes: the "base" and the "lid". The 19S base complex consists of the six AAA-family ATPases that interact with alpha subunits of the 20S proteasome and non-ATPases that bind to polyubiquitin conjugates. The 19S regulator lid complex is made up of eight non-ATPase subunits and is proposed to be essential for polyubiquitin substrate processing prior to degradation (*12*). Mammalian cells and the protozoan *Trypanosoma brucei* also contain an ATP-independent activator of the 20S proteasome (or 11S regulator), named the PA28 or PA26 complex, respectively (*18, 19*). However, the 11S regulator is absent in yeast. PA28 and PA26 complexes activate degradation of small peptides but not ubiquitinated proteins (*18, 19*). The PA28 activator is a 200-kDa ring-shaped

† This work was supported by a grant from the National Institutes of Health to V.N. and by fellowships from Ministerio de Educación y Cultura of Spain to J.L.D. and the Pew Latin American Fellows Program to J.G.

* To whom correspondence should be addressed: Michael Heidelberger Division MSB 134, Pathology Department, New York University School of Medicine, 550 First Ave., New York, NY 10016. Telephone: +1-212-263-7870. Fax: +1-212-263-8179. E-mail: diegoj01@med.nyu.edu.

New York University School of Medicine.

§ University of California.

‡ University of Antofagasta.

10.1021/bi001659k CCC: $20.00
Published on Web 01/03/2001

heteromultimer composed of two isoforms of a 28-kDa subunit (PA28α and PA28*β*) and is present in the cytoplasm as a free complex or associated with the proteasome. The PA28 complex is inducible by *γ*-interferon and is required for efficient antigen processing and also for immunoproteasome assembly (*20*). The function of PA26 complex in *T. brucei* is unknown.

We have previously reported that lactacystin, a highly specific inhibitor of the 20S proteasome (*21*), inhibits trypomastigote transformation both in culture medium and within cells (*22*). In another protozoan parasite, *T. brucei*, lactacystin inhibits the proliferation of both the mammalian and the insect forms, and arrests them in the G2+M and G1/S phase, respectively (*23*). The 20S core has been successfully isolated from several protozoan parasites, including *T. brucei*, but the presence of the 26S proteasome and the participation of the ubiquitin pathway in protein degradation has not been documented in protozoa. In fact, it has been suggested that trypanosomes lack the 26S proteasome, and the 20S proteasome is only activated by the PA26 complex (*24*). Since, the PA26-activated 20S proteasomes do not degrade proteins (*19*), this implies that the bulk of protein turnover in trypanosomes is not via the Ub−proteasome system and might operate similar to bacteria without the benefit of ubiquitination. Archea and prokaryotes contain ATP-dependent proteases that share remarkable structural and funtional similarity with the eukaryotic 26S proteasome (*15*). Although bacterial proteasomes can recognize linear peptide degradation signals within proteins (class I degrons), during evolution, the eukaryotic proteasome acquired the additonal capacity to recognize a multiubiquitin chain (*16*). In the present study, we have used the tripanosomatid parasite *T. cruzi* to explore the participation of the Ub−proteasome system in protein degradation during the time of parasite remodeling.

EXPERIMENTAL PROCEDURES

Materials. Protease inhibitors, fluorogenic substrates, and other reagents were purchased from Sigma Chemical Co. (St. Louis, MO), except as otherwise noted. Calpeptin (benzyloxycarbonyl-Leu-norleucinal) (Cbz-Leu-norleucinal) was from Calbiochem (La Jolla, CA). Radiochemicals and Chemical Luminescence kit were from Amersham Pharmacia Biotech, Inc (Piscataway, NJ).

Protein Turnover in Live Parasites. LLC-MK_2 cells were infected with *T. cruzi* trypomastigotes, Y strain. Five days later, the supernatants contained more than 90% trypomastigotes. The parasites were centrifuged, washed with DMEM medium (1% dialyzed-FCS, 10 mM HEPES, pH 7.4), and incubated in the same medium without leucine and isoleucine for 45 min at room temperature. To measure the breakdown of short-lived protein, 2.0×10^7 trypomastigotes/mL were metabolically labeled for 1 h at room temperature with 0.5 μCi/mL ^{14}C-leucine in the presence or absence of one of the following protease inhibitors: 30 μM lactacystin, 10 mM methylamine, 25 μM calpeptin, 30 μM E-64d, 30 μM leupeptin, 50 μM vinyl sulfone (Z-L3VS),[1] or 25 μM CBZ-Phe-Ala-FK. At the end of this period, parasites were washed three times to remove extracellular ^{14}C-leucine and resuspended in DMEM, pH 7.4, containing 0.4% BSA, 20 mM HEPES, and 0.5 mg/mL cold leucine. Aliquots corresponding to time 0 were taken. The remaining trypomastigotes were incubated at 37 °C, in the presence or absence of the above-mentioned protease inhibitors, either in DMEM, pH 7.4, or in transformation medium (DMEM, pH 5.0) to trigger trypomastigote transformation into amastigotes (*4*). Samples were taken at indicated times. To measure protein degradation, the samples were chilled for 1 h on ice in 10% trichloroacetic acid and centrifuged for 3 min at 20000*g*. The radioactivity in the TCA soluble and insoluble materials was measured using a Beckman LS 5000TD counter. Protein degradation was expressed as the percentage of incorporated radioactivity that had been converted into the acid-soluble form. To measure the breakdown of long-lived proteins, fourth-day *T. cruzi*-infected cell cultures were labeled with ^{14}C-leucine for 18 h at 37 °C. Trypomastigotes obtained from the culture supernatants were incubated in chase medium (DMEM, 20 mM HEPES, 0.4% BSA, 0.5 mg/mL leucine) for 1 h at 37 °C in the presence or absence of inhibitors. Measurement of protein degradation was performed as above.

ATP-Dependent Proteolysis Assays. After metabolic labeling, ATP production was blocked by preincubation for 1 h in DMEM, pH 7.4, containing 25 mM 2-deoxyglucose instead of glucose and 2.5 mM ATPγS (a non-hydrolyzable ATP analog) in the presence or absence of a cocktail of inhibitors detailed in Figure 3 legend. Parasites were transferred to transformation medium (pH 5.0) containing the same inhibitor composition and incubated for an additional 2 h. At the end of the incubation, parasites were centrifuged and rapidly frozen. To measure protein degradation, samples were processed as described above. ATP determination was performed by the luciferase−luciferin assay. Further details are in the figure legend.

Assays for Protein Ubiquitination. To detect ubiquitinated proteins by Western blot, 5×10^6 trypomastigotes were washed twice in PBS, centrifuged, and incubated both at low pH (pH 5.0) and at physiological pH for indicated times. After incubations, parasites were washed in PBS and centrifuged at 3500*g* for 6 min. The resulting pellet was resuspended in a lysis buffer containing 50 mM Tris-HCl, 150 mM NaCl, 1% CHAPS, 50 μM E-64, 10 mM EDTA, 5 mM NEM, 1 mM PMSF, 10 μg/mL leupeptin, and 10 μg/mL aprotinin. After 20 min on ice, 10 μg of crude lysate was loaded onto SDS−PAGE and blotted onto PVDF membranes. Protein quantification was measured by BCA protein assay (Pierce, Rockford, IL). Ubiquitin conjugates were detected using a specific anti-ubiquitin mAb (Zymed Laboratories Inc, San Francisco, CA) and a anti-mouse IgG-peroxidase conjugate. Blots were developed using Enhanced Chemical Luminescence system. To detect the accumulation of ubiquitinated proteins in trypomastigotes, the parasites were pretreated with 30 μM lactacystin or as controls with 30 μM E-64d, 30 μM calpeptin, or 25 mM 2-deoxyglucose in DMEM, pH 7.4, at 37 °C for 1 h. Parasites were transferred to DMEM, pH 5.0, containing the same inhibitor composition as in the previous step, and incubated for an additonal 2 h. Ubiquitinated proteins were detected as above.

[1] Abbreviations: Amc, 7-amino-4-methylcoumarin; E-64d, (2*S*,3*S*)-*trans*-epoxysuccinyl-L-leucyl-amido-3-methylbutane ethyl ester; mAb, monoclonal antibody; PAR, paraflagellar rod protein; PVDF, poly(vinylidene difluoride); Z-L3VS, leucyl-leucyl-leucine vinyl sulfone; Ub, ubiquitin.

Assay for Ubiquitination of Cytoskeletal Proteins in the Flagellar Fraction. To trigger remodeling, *T. cruzi* trypomastigotes were incubated in transformation medium (pH 5.0). In some experiments, the parasites were preincubated with 25 μM lactacystin for 45 min at pH 7.4 and subsequently incubated in transformation medium (pH 5.0) in the presence of lactacystin at the same concentration. Aliquots containing 2.8×10^7 were taken at time 0 (pH 7.4) and 1, 2, 3, and 4 h later in transformation medium (pH 5.0). For the ubiquitin conjugation assays, parasites were washed once with PBS and then permeabilized with 50 μL of buffer containing 0.2% NP-40, 40 mM Tris-HCl, pH 7.5, 50 μM E-64, and 2 mM DTT. ^{125}I-ubiquitin was then added, and the permeabilized parasites were incubated at 37 °C for 25 min in the presence or absence of lactacystin (25 μM), either in ATP-depleted medium that contained 0.5 μg hexokinase, 10 mM 2-deoxyglucose, and 1 U apyrase, or in a medium containing an ATP-regenerating system, which contained 5 mM $MgCl_2$, 5 mM ATP, 10 mM creatine phosphate, and 10 μg of creatine kinase. The reaction was stopped by centrifugation at 15000*g* for 10 min at 4 °C. The parasite's cytoskeletal flagellar fraction was extracted from the pellets (*25*) by incubation with buffer A (60 mM PIPES, 25 mM HEPES, 10 mM EGTA, 2 mM $MgCl_2$, 0.5% Triton X-100, 50 μg/mL antipain, 10 μg/mL aprotinin, 10 μg/mL E-64, 5 μg/mL leupeptin, 10 μg/mL pepstatin A, 1 mM PMSF, 50 mM NaF, 20 mM sodium pyrophosphate, and 2.5 mM orthovanadate). The resulting cytoskeleton proteins were washed twice in buffer A and extracted with buffer A containing 1 M NaCl, and the resulting material was dissolved with 6 M urea for 1 h on ice. As determined by Coomassie blue staining of SDS gels, this fraction contained almost exclusively paraflagellar rod proteins and tubulins. Radioactivity was evaluated in a LKB 1260 Multigamma Counter.

26S Proteasome Purification. All purification steps were carried out within 48 h, and none of the intermediate fractions were frozen. *T. cruzi* epimastigotes were harvested from 3 L of culture and washed three times in PBS. The resulting pellets were homogenized in buffer B (25 mM Tris-HCl, pH 7.5, 1 mM EDTA, 2 mM ATP, 1 mM DTT, and 5 mM $MgCl_2$) and 0.25 M sucrose. Parasites were disrupted on ice using a nitrogen cavitation bomb (600 psi for 5 min), and the homogenate was spun for 1 h at 100000*g*. The supernatant was supplemented with 3 mM ATP and loaded onto a hydroxylapatite column equilibrated with 10 mM sodium phosphate buffer, pH 6.8, containing 1mM DTT, 5 mM ATP, and 20% glycerol. The fractions containing 26S were loaded directly onto a DEAE Affigel Blue (BioRad Labs., Hercules, CA) column equilibrated with buffer C (buffer B containing 10% glycerol). After the column was washed with 40 mM KCl in buffer C, the 26S proteasomes were eluted with 0.2 M KCl in buffer C. Fractions were concentrated using Millipore Ultrafree filters and fractionated by Fast Performance Liquid Chromatography using Superose 6 HR 16/30 equilibrated with 50 mM Tris-HCl, pH 7.5, 1 mM DTT, 2 mM ATP, 5 mM $MgCl_2$, 0.1 M KCl, and 10% glycerol. Fractions were assayed for peptidase activity using the fluorogenic substrate Suc-LLVY-Amc as described below. A pool of the peak fractions containing 26S were subjected to nondenaturing gel electrophoresis, followed by fluorogenic peptide overlay as described below. Purified 26S proteasomes were analyzed by Western blot using a monoclonal antibody to the α-subunit of *T. cruzi* 20S (mAb 7E5)[2] and antibodies against members of the AAA family of ATPases present in 26S proteasomes (Affiniti Research Product, Exeter, U.K.). The antibodies were against yeast subunit YTA-1 (homologue to human S6a), human subunit TBP-7 (S6b), human subunit p45 (S5), human subunit MSS1 (S7), yeast subunit YTA-5 (homologue to human S4). Yeast 26S proteasomes were partially purified as in ref *26* from 1 L of yeast cells (Y190). Preparation of yeast protein extract was done from a spheroplast preparation and lysis using Dounce homogenization in 50 mM Tris-HCl, pH 7.5, 1 mM DTT, 2 mM ATP, 5 mM $MgCl_2$, and 20% glycerol. Two milligrams of yeast lysate was loaded onto 10 mL of 15−35% glycerol density gradient in 20 mM Tris-HCl, pH 7.5, 1 mM DTT, and 2 mM MgATP. After centrifugation at 28000 rpm for 18 h at 4 °C in a SW41 rotor (Beckman, USA), the gradient was separated into 300-μL linear sample fractions and assayed for peptidase activity against Suc-LLVY-Amc. The peak fractions containing the 26S proteasome were pooled, kept with 1 mM ATP and 20% glycerol, and stored at −80 °C until use.

Peak fractions containing the 26S or 20S proteasome activities were initially recognized by their ability to hydrolyze 100 μM of Suc-LLVY-Amc in 50 mM Tris-HCl, pH 7.5, 1 mM DTT, and 50 μM E-64. The fractions containing the 26S proteasome were identified by the ATP-mediated stimulation of hydrolytic activity in the presence of 2 mM ATP and 5 mM $MgCl_2$ and by the inhibitory activity of 0.02% SDS. In contrast to the 26S proteasome, the activity of the 20S proteasome is enhanced by incubation with 0.02% SDS (*27*). To deplete ATP, samples contained 1 U of apyrase. To measure peptidase activity, 10 μL of sample fractions were added to 90 μL of appropriate fluorogenic peptide solution, and the mixtures were incubated at 37 °C for 30−60 min before quenching with 200 μL of cold ethanol. Fluorescence was recorded in a Fluoroskan II (Labsystem, Helsinski, Finland) using an excitation wavelength of 380 nm and an emission wavelength of 440 nm (*27*).

Nondenaturing Gel Electrophoresis and Substrate Overlay. Purified proteasomes were resolved in 4% nondenaturing PAGE as described (*17*). Briefly, a single gel layer was made up with 4% acrylamide-*N*,*N*′-bisacrylylcystamine (at a ratio of 22:1), 0.18 M Tris-borate, pH 8.3, 5 mM $MgCl_2$, 1mM ATP, 1mM DTT, and polymerized with 0.1% TEMED and 0.1% ammonium persulfate. The running buffer was the same as the gel buffer but without acrylamide. Proteins were resuspended in a loading buffer containing 50 mM Tris-HCl, pH 6.9, 5% glycerol, and xylene cyanol. Nondenaturing minigels were run at 100 V at 4 °C until the xylene cyanol eluted from the gels. The gels were then incubated in 5 mL of 0.1 mM Suc-LLVY-Amc in 50 mM Tris-HCl, pH 7.5, 5 mM $MgCl_2$, 10% glycerol, 1 mM ATP, 1 mM DTT, and 50 μM E-64. Proteasome bands were visualized upon exposure to UV light and photographed with a Polaroid Camara using a Kodak purple gelatin filter No. 34A. In some cases, the proteolytically active bands were cut out of the gels and incubated with 40 μL of 2 M DTT per 100 μL of gel slice for 30 min at 30 °C. Laemmli loading buffer was added to

[2] J. González, unpublished data.

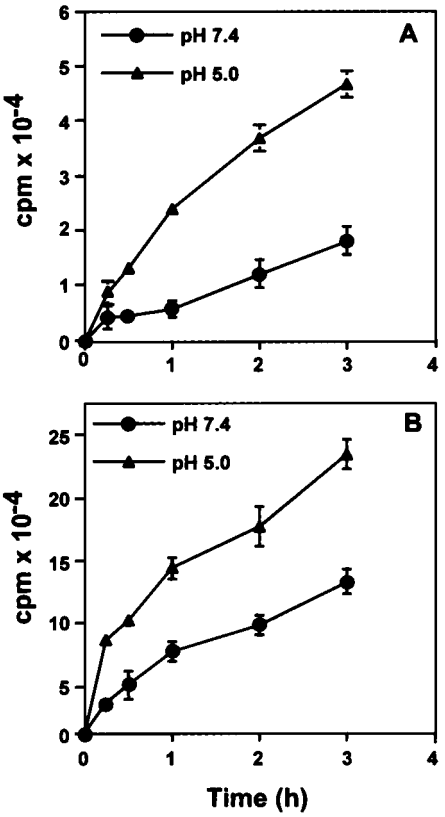

FIGURE 1: Turnover of intracellular protein during *T. cruzi* remodeling. Trypomastigotes were metabolically labeled with ^{14}C-leucine during 1 or 18 h for short-lived (panel A) and long-lived (panel B) proteins, respectively. After taking a sample at time 0, parasites were incubated either in DMEM, pH 7.4, or DMEM, pH 5.0, for an additional 1, 2, or 3 h. Protein breakdown was measured as the release of ^{14}C-leucine counts by TCA precipitation. The data shown are the mean values and standard deviations obtained in three independent experiments and indicate the counts released into the supernantant at pH 7.4 (solid circle) and at pH 5.0 (solid triangule).

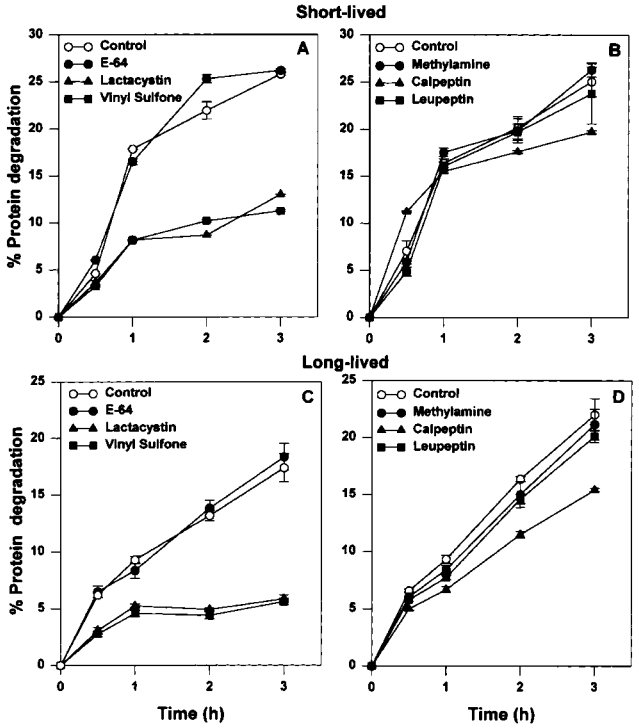

FIGURE 2: Degradation of both short-lived and long-lived protein during remodeling of *T. cruzi*. Trypomastigotes were metabolically labeled as described in Figure 1. For short-lived proteins, trypomastigotes were preincubated with specific proteasome inhibitors (panel A) or different protease inhibitors (panel B) during the metabolic labeling. For long-lived proteins, 18 h-^{14}C-leucine labeled-trypomastigotes were chased for 1 h with DMEM, pH 7.4. During the chase, parasites were incubated with specific proteasome inhibitors (panel C) or different protease inhibitors (panel D). For either long- or short-lived proteins, aliquots were collected at time 0, 0.5, 1, 2, and 3 h, and protein degradation was evaluated by TCA precipitation. The data shown here are expressed as mean ± SE (n = 3) and represent the percent of protein degradation. Inhibitor concentrations are lactacystin (30 μM), calpeptin (25 μM), Z-L3VS or vinyl sulfone (50 μM), E-64d (30 μM), leupeptin (30 μM), and methylamine (10 mM).

the samples, boiled for 5 min, and loaded onto 10% SDS gels. Proteins were detected by ammoniacal-silver staining.

RESULTS

Role of Proteasome in Protein Breakdown during Transformation. We initially compared the rates of protein degradation when trypomatigotes are triggered to transform into amastigotes by acidic medium (pH 5.0) versus those maintained at pH 7.4. Short- and long-lived proteins were arbitrarily defined by metabolic labeling of trypomastigotes for 1 and 18 h, respectively, and protein turnover was measured at pH 7.4 and pH 5.0. In several independent experiments, protein breakdown was consistently higher in parasites maintained at the lower pH (Figure 1). The differences were more striking for comparisons made between the rates of breakdown of short-lived (Figure 1, panel A) versus long-lived proteins (Figure 1, panel B). After 2 h of incubation at pH 5.0 or pH 7.4, 19.6 versus 13.9%, respectively, of short-lived proteins were degraded and 14 versus 10.7%, respectively, for long-lived proteins.

Short-lived protein degradation exhibited biphasic kinetics, suggesting that the labeled proteins are composed of a heterogeneous population of molecules with different half-lives. To study the contribution of the lysosomal and proteasomal pathways, trypomastigotes were treated with specific inhibitors (Figure 2). The breakdown of short-lived protein was inhibited by 55−60% in the presence of specific and irreversible proteasome inhibitors such as lactacystin and Z-L3VS, a tripeptide vinyl sulfone (Figure 2, panel A). Methylamine and leupeptin had little or no inhibitory effect (<10%) (Figure 2, panel B). Even at a concentration of 30 μM, E-64d had no detectable effect on protein turnover (Figure 2, panel A). Among cysteinyl protease inhibitors, only calpeptin (an inhibitor of calpains) had a moderate inhibitory effect on short-lived protein degradation (20 ± 2%) (Figure 2, panel B). However, it has been reported that high concentrations of calpeptin (100 μM) may also inhibit some mammalian proteasome peptidase activities (*29*). In an attempt to identify whether the proteasome is a target of calpeptin in *T. cruzi*, we studied the inhibitory effect of calpeptin on the proteolytic activities of immunopurified proteasomes from calpeptin pretreated parasites at 30 μM at low pH for 2 h. No inhibition in any 20S peptidase activities was observed (not shown). Moreover, in several experiments, we included both calpeptin and lactacystin in the transformation medium. We consistently observed an additive effect: after 2 h of incubation at pH 5.0, lactacystin inhibited protein breakdown by 55%, while 75% of protein degradation was

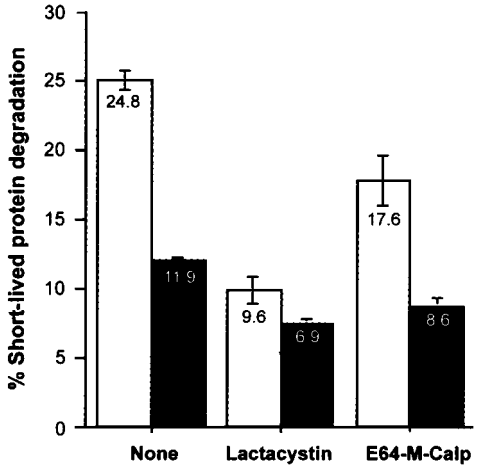

FIGURE 3: Inhibition of ATP production blocks rapid short-lived protein breakdown during transformation. 2.0×10^7/mL labeled trypomastigotes were preincubated for 1 h in the presence or absence of either lysosomal and Ca^{2+}-dependent protease inhibitors (10 mM methylamine, 30 μM E−-64d, and 25 μM calpeptin) or lactacystin 30 μM (clear bars). At the same time, another set of trypomastigotes were preincubated in a glucose-free DMEM containing the above-mentioned inhibitors and supplemented with 25 mM 2-deoxyglucose and 2.5 mM ATPγS to block and replace ATP levels, respectively (darkened bars). Parasites were later transferred to DMEM, pH 5.0, containing the same inhibitor composition as above, and incubated for an additional 2 h. The percent protein degradation is shown.

inhibited in the presence of both calpeptin and lactacystin (not shown).

The results obtained for long-lived protein degradation were similar. Lactacystin and Z-L3VS were the strongest inhibitors (70−74%). Lysosomal cysteinyl protease inhibitors were poor inhibitors (10−15%), while calpeptin inhibited protein degradation by 30% (Figures 2, panels C and D). Therefore, we conclude that the protein breakdown during trypomastigote remodeling takes place mainly in the proteasome, with some participation of calpain-like activity but not of lysosomal enzymes.

Short-Lived Protein Degradation by Proteasomes Requires ATP. To determine whether the degradation of short-lived proteins is ATP-dependent, we initially incubated trypomastigotes in glucose-free-medium containing 2-deoxyglucose to deplete ATP as described elsewhere. This condition reduced the ATP content in trypomastigotes by 60−65% and protein degradation by 27%. Since *T. cruzi* is capable of utilizing both carbohydrates and amino acids to supplement its energy requirements (*30*), we targeted the ATP-dependent protein degradation by incubating trypomastigotes in glucose-free medium containing 2-deoxyglucose and ATPγS to partial deplete and replace intracellular ATP, respectively. After this treatment, the parasites remained alive, but protein degradation was reduced by 52 ± 0.5% (Figure 3). ATPγS has been reported to inhibit ubiquitin-dependent proteolysis in vitro (*31*) and is known to bind ATP receptors in mammalian cells (*32*). A membrane receptor-mediated ATP transport system has been identified in *T. cruzi* trypomastigotes (*33*). It is conceivable that ATPγS might bind to this transporter and enter the cytoplasm of trypomastigotes. Treatment with ATPγS alone reduced protein degradation by 25%, but total ATP content could not be evaluated, most likely because the incorporated ATPγS interfered with our ATP quantification assay. It is noteworthy that the ATPγS-mediated interference appeared more pronounced with the addition of 2-deoxyglucose in the ATPγS-treated parasites. Next, we attempted to identify the proteolytic pathways affected by 2-deoxyglucose and ATPγS mediated-ATP depletion. Parasites were pretreated with medium containing either protease inhibitors or a mixture of inhibitors with 2-deoxyglucose and ATPγS. In parasites treated with lactacystin, protein degradation was strongly inhibited (61 ± 0.8%), and addition of 2-deoxyglucose and ATPγS had a minimal effect. In parasites treated with methylamine, E-64d and calpeptin to inhibit lysosomal and Ca^{2+}-dependent proteolysis, degradation was inhibited by 29 ± 1%. The addition of 2-deoxyglucose and ATPγS inhibited degradation by an additional 51 ± 1.2%. These results strongly suggest that ATP-depletion affected mainly or exclusively the proteasome pathway.

Ubiquitination of Proteins Increases during Trypomastigote Transformation into Amastigote. To detect ubiquitination of proteins during transformation, we performed Western blots using specific antibodies to ubiquitin. As shown in Figure 4, there is a strong increase in the levels of ubiquitinated proteins in total extract of parasites incubated in transformation medium (pH 5.0). We reasoned that if ubiquitination is required for the degradation of proteins by the proteasome, the presence of lactacystin during transformation should lead to an accumulation of ubiquitinated proteins. This was in fact observed, as shown in Figure 4, panel B. The effect was lactacystin-specific and was not observed after incubation of parasites in the presence of E-64d or calpeptin. Ubiquitin conjugation was suppressed when trypomatigotes were depleted of ATP by incubation in glucose-free medium containing 2-deoxyglucose (Figure 4, panel B).

Isolation of the T. cruzi 26S Proteasome. Purification of the 26S proteasome of *T. cruzi* epimastigotes was carried out by series of chromatographic steps including hydroxylapatite, DEAE affigel-blue, and Superose 6 columns. The elution profile of the superose columns is shown in Figure 5, panel A. A high molecular weight proteolytic complex with chymotrypsin-like activity against the substrate Suc-LLVY-Amc was identified. Its activity was enhanced 2−4-fold by 2 mM ATP and was totally inhibited by incubation with 0.02% SDS. A second peak of acitivity with a smaller molecular size contained the proteasome core, and its chymotryptic activity was greatly enhanced by treatment with SDS (Figure 5, panel A). On the basis of its elution profile from Superose 6 (Figure 5, panel A) and electrophorectic migration in nondenaturating gels (Figure 5B), the large complex has a molecular mass of ∼1400 kDa, a 2.2-fold increase in the molecular mass of *T. cruzi* 20S proteasome. When the nondenaturing gels were overlayed with the fluorogenic substrate Suc-LLVY-Amc, the complex migrated as a single spot, and in a position identical to the 26S proteasome isolated from yeast (Figure 5, panel B). The 26S band was cut out from the nondenaturing gel and subjected to SDS−PAGE. About 30 proteins in a range of 25−110 kDa were observed after silver-staining (Figure 5, panel C), including the 20−35 kDa subunits of the 20S core. Components of purified *T. cruzi* 26S were specifically recognized by Western blot using antibodies raised against the AAA family of ATPases (ATPases Associated with a variety of

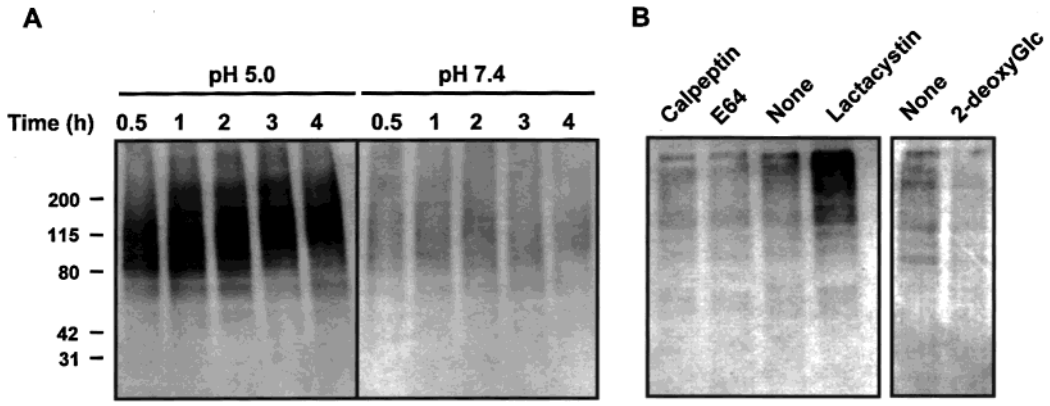

FIGURE 4: Increase of ubiquitin conjugated protein levels during *T. cruzi* remodeling. Panel A, 5×10^6 trypomastigotes were incubated at pH 5.0 or at physiological pH 7.4 for 0.5, 1, 2, 3, and 4 h. After incubations, parasites were centrifuged and resuspended in lysis buffer as described in Experimental Procedures. Ten micrograms of total protein was resolved in 4−15% SDS−PAGE. After transfer of proteins, ubiquitin conjugates were detected using anti-ubiquitin mAb. Panel B, trypomastigotes were preincubated at 37 °C for 1 h with either 30 μM E-64d, 30 μM calpeptin, 30 μM lactacystin, 25 mM 2-deoxyglucose, or alone in DMEM, pH 7.4. Parasites were transferred to transformation medium (pH 5.0) containing the same inhibitor composition for an additional 2 h. Five micrograms of total protein was resolved in 10% SDS−PAGE and short time exposures were taken to visualize better the increase in the levels of ubiquitinated proteins in the presence of lactacystin. Western blot was processed as described in panel A. Molecular weight markers are shown in kilodaltons.

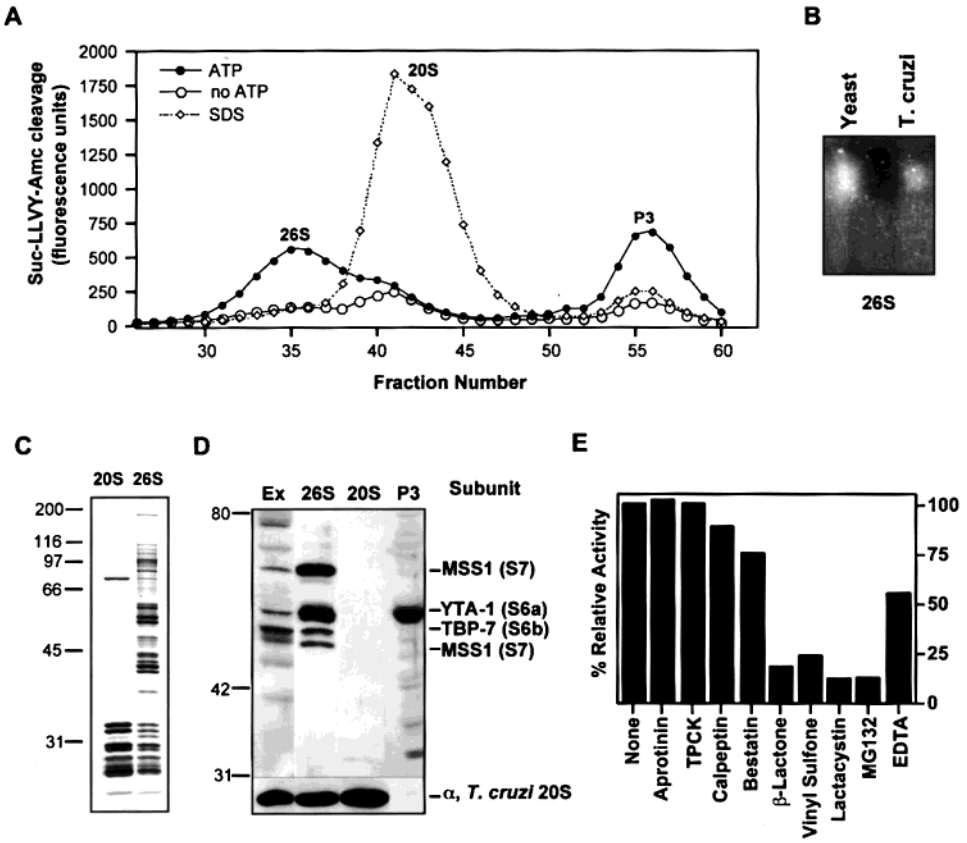

FIGURE 5: Proteolytic activity of fractions eluted from the Superose 6 column. Panel A, proteolytic activity was monitored by enzymatic cleavage of Suc-LLVY-Amc in the presence or absence of MgATP. Other samples were assayed with SDS in the absence of ATP. Panel B, 26S fractions analyzed by nondenaturing PAGE, followed by overlay with the peptide Suc-LLVY-Amc in the presence of ATP. Panel C, SDS−PAGE silver stain of the *T. cruzi* 26S band shown in Panel B. Panel D, reactivity of proteasome ATPases from purified *T. cruzi* 26S proteasomes and from a pool fraction containing the peak3 (P3) by polyclonal antibodies anti-yeast YTA1 (or human S6a), human MSS1 (S7), and human TBP-7 (S6b). The *T. cruzi* 20S proteasome was detected by reactivity using a monoclonal antibody 7E5 against α-subunits[2] after stripping the membrane. Panel E, the influence of inhibitors on the degradation Suc-LLVY-Amc by *T. cruzi* 26 S was measured in the presence of 2 mM ATP, 5 mM $MgCl_2$, and 50 μM E64. 100% degradation is taken for the peptidase activity obtained in the presence of ATP/$MgCl_2$. Inhibitor concentrations used are aprotinin (5 μg/mL), TPCK (0.1 mM), calpeptin (30 μM), bestatin (0.1 mM), β-lactone (10 μM), vinyl sulfone (30 μM), lactacystin (30 μM), MG132 (30 μM), and EDTA (10 mM). Percentage of relative peptidase breakdown is shown.

cellular Activities) from eukaryotic 26S proteasome (*34*). Anti-yeast YTA-1 (or human S6a), anti-human TBP-7 (S6b), and anti-human MSS1 (S7) strongly recognized bands of 50−60 kDa (Figure 5, panel D). In fact, it has been recently reported that an expressed sequence tag cDNA in *T. cruzi* epimastigote EST's databases shares homology with the

human S6a (AI066170)[3]. Antibodies against the *T. cruzi* 20S proteasome also recognized the purified *T. cruzi* 26S proteasome (Figure 5, panel D). Specific inhibitors of the proteasome such as lactacystin, β-lactone, and vinyl sulfone (ZL3VS) inhibited the activity of the *T. cruzi* 26S proteasome. Bestatin (endopeptidase inhibitor), TPCK, and aprotinin (serine protease inhibitors) had no effect (Figure 5, panel E).

As also shown in Figure 5, panel A, we detected a small peak of estimated molecular weight of 150 kDa (peak 3) with an ATP-dependent proteolytic activity against Suc-LLVY-Amc. Although its presence was confirmed in additional experiments, the activity was rapidly lost and further attempts at characterization were not successful, suggesting that more than one factor might be required for activity. The pool fraction of that peak3 (P3) was not recognized by antibodies to *T. cruzi* 20S α-subunits but reacted with anti-yeast YTA-1 antibodies (Figure 5, panel D). It leads us to suggest that this peak might contain a member of the AAA family of ATPases unless it is part of the disassembly of 19S cap. Perhaps, this smaller enzyme is a part of one of the ATP-dependent proteases described in prokaryotes and in mitochondria of eukaryotic cells (FtsH, Lon, ClpAP, and ClpXP) (*35*).

Cytoskeletal Proteins from the Flagellar Fraction Are Ubiquitinated in Permeabilized Parasites Incubated at pH 5.0. When trypomastigotes undergo transformation to amastigotes, most of the flagellar structure disappears. As shown above, during this process, many proteins are ubiquitinated. To determine whether flagellar proteins are among them, we performed ubiquitin conjugation assays in permeabilized parasites since exogenous ubiquitin (8.6 kDa molecule) does not enter the living parasite. Radiolabeled ubiquitin was added to the permeabilized parasites under different conditions, and flagellar proteins were extracted at different time points. As shown in Figure 6, panel A, a basal level of ubiquitin conjugation was observed in trypomastigotes kept at pH 7.4. A strong increase in ubiquitin conjugation was noted in trypomastigotes incubated between 1 and 2 h at pH 5.0 in the presence of ATP. In the absence of ATP, no change in the level of ubiquitination was observed at either pH 7.4 or pH 5.0. Samples from similar preparations were analyzed by SDS−PAGE. As shown in Figure 6, panel B, they contained mainly paraflagellar rod proteins (PAR) and tubulins. Also shown is the gradual disappearance of PAR during incubation at pH 5.0 in the presence of MgATP and the inhibitory effect of lactacystin. The radioautography is shown in Figure 6, panel C. As shown, ubiquitination is ATP-dependent. In the presence of lactacystin, a smear containing accumulated ubiquitinated protein is observed. The molecular masses vary between 60 kDa and greater than 200 kDa. Although there is a correlation over time between the disappearance of PAR and the accumulation of ubiquitinated proteins, we could not directly identify ubiquitinated PAR under these experimental conditions (data not shown).

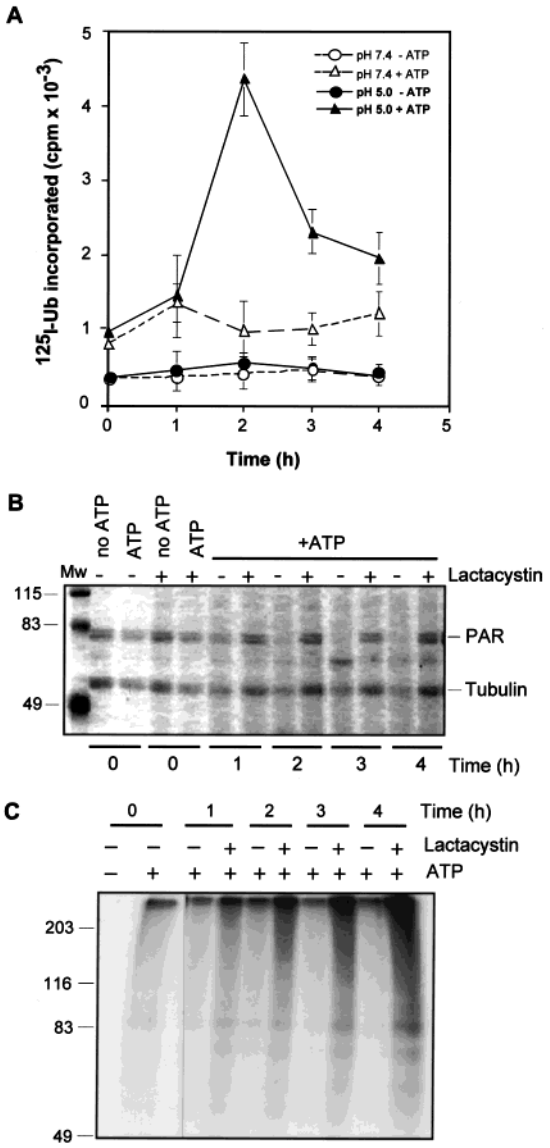

FIGURE 6: Conjugation of ^{125}I-ubiquitin to cytoskeletal flagellar proteins during transformation. *T. cruzi* trypomastigotes were incubated at pH 7.4 or pH 5.0 for indicated times. For the ubiquitin conjugation assays, 2.8×10^7 parasites were permeabilized with 50 μL of conjugation buffer containing 0.2% NP-40 and incubated with ^{125}I-ubiquitin at 37 °C for 25 min in the presence or absence of ATP. Identical samples were incubated under the same conditions in the presence or absence of lactacystin. Parasites were centrifuged and pellets were submitted to extraction of cytoskeletal flagellar proteins as described in Experimental Procedures. Panel A, conjugation of ubiquitin was evaluated in a γ counter and expressed as cpm. The data shown represent the mean values and standard deviations obtained in three independent experiments. Panel B, Coomassie staining of the gel of the preparations described above. Panel C, autoradiography of the ubiquitin conjugation assay.

DISCUSSION

Although the presence of the 20S proteolytic core has been demonstrated in a broad range of organisms, including *T. cruzi* (*22*), *T. brucei* (*36*, *37*), *Leishmania mexicana* (*38*), *Giardia lamblia* (*39*), *Entamoeba invadens* (*40*), and *Entamoeba histolytica* (*41*), the 26S proteasome has not been identified in any protozoan. Trypanosomatid protozoan parasites represent one of the earliest branches in eukaryotic lineage using molecular phylogenetic analysis (*28*). Because of the lack of evidence of an ATP/Ub-dependent proteolytic system in these parasites, it has been suggested that proteasome degradation may be similar to prokaryotes. We explored that hypothesis using the tripanosomatid *T. cruzi* and we identified the 26S proteasome of *T. cruzi* epimas-

[3] Accession number.

tigotes as a high molecular weight complex (1400 kDa) with composition that resembles that of the 26S proteasome isolated from other eukaryotic cells. We identified tentatively some members of the AAA family of ATPases present in the 19S complexes that cap the 26S proteasomes and that are highly conserved (*42*). In Western blots of *T. cruzi* 26S, the subunits S6a (p50, YTA1), S6b (p48, TBP7), and S7 (MSS1) ATPases members revealed strong bands with the expected molecular mass. During self-assembly of the 19S regulatory complex, the ATPases are paired (S6a binds to S10b, S6b binds to S8, and S7 binds to S4) (*43*), suggesting that the S4, S8, and S10b subunits may also be present in the 26S proteasome of *T. cruzi*. Sequences with homology to S6a and other components of the *T. cruzi* 26S proteasome have been reported in the database (S6a, AI066170; S14 or P31, AI069659; S2, AI612566).[3]

The rate of degradation of intracellular proteins increases substantially when trypomastigotes are shifted to pH 5.0. Concomitant with this pH shift, a large proportion of the intracellular protein breakdown is degraded via an ATP-dependent proteasome. In mammalian cells, the turnover of short-lived proteins (which control key regulatory processes such as signal transduction) and long-lived proteins is mediated mainly by the Ub−proteasome system (*44*, *45*). It is conceivable that the observed acceleration of protein turnover at pH 5.0 may be due to the degradation of proteins involved in signal transduction pathways during *T. cruzi* remodeling. Participation of the ubiquitin pathway in protein degradation in *T. cruzi* is suggested by the strong increase in the levels of ubiquitinated proteins when trypomastigotes transform into amastigotes (Figure 4). Furthermore, depletion of endogenous ATP in trypomastigotes abrogated ubiquitin conjugation and reduced considerably the breakdown of short-lived proteins (Figure 3). When proteasome activity is abolished during transformation, an accumulation of ubiquitinated proteins is observed. The *T. cruzi* genome contains more than 100 ubiquitin-coding sequences, a number much larger than in other organisms (*46*). Heat-shock elements whose transcription is altered under stress conditions are present in the intergenic regions preceding the polyubiquitin genes (*47*). It is conceivable that their expression is upregulated when the parasite reaches the acidic environment of the endosomal compartment, immediately following cell invasion (*1*). In *Plasmodium falciparum*, another parasite that undergoes striking host and stage-specific transformations, heat shock responses are associated with slightly elevated levels of ubiquitin transcripts, and increases in the amounts of polyubiquitinylated proteins (*48*).

Consistently, a calpain-like activity had a minor role in protein turnover during parasite remodeling. Although calpain has not been identified so far in protozoan parasites, several genes with homology to calpain have been reported in trypanosomes (T26731, AQ901910 and AQ852527),[3] and indirect evidence for the presence of the enzymatic activity has been observed (*49*−*51*). In mammalian cells, calpain activity is modulated by Ca^{2+} concentration, and one of its functions is to cleave intracellular structural proteins (*52*, *53*). A similar role could be envisaged for the putative *T. cruzi* calpain, i.e., it may participate in the turnover of cytoskeletal proteins during transformation of trypomastigotes into amastigotes. Perhaps of relevance, calcium fluxes within the trypomastigotes are detected during entry into host cells, and the concentration of intracellular Ca^{2+} is greater in amastigotes than in trypomastigotes (*54*−*56*).

Little is known about the involvement of the proteasome in the diverse biological functions of other protozoan parasites. Lactacystin at nanomolar concentrations inhibits the development of the exoerythrocytic and erythrocytic stages of *Plasmodium* (*57*) and encystation of *E. invadens* (*40*). In *T. brucei*, lactacystin-treated bloodstream forms differentiate normally into procyclic forms, and intracellular levels of several glycosomal enzymes remained unchanged during differentiation (*58*). However, the remodeling of *T. brucei* does not involve morphological changes as dramatic as *T. cruzi*. In fact, it is not clear whether *T. brucei* remodeling represents conventional eukaryotic differentiation (*58*).

It has been proposed that protein degradation in *T. brucei* may operate as in prokaryotes, since attempts to identify the 26S proteasome in *T. brucei* have not been successful. Instead, *T. brucei* (but apparently not *T. cruzi* or *Leishmania*) contains a potent activator of the 20S proteasome named PA26. The properties of PA26 resemble in some ways those of PA28α, the activator of the 20S of mammalian cells, that is absent in yeast. The function of PA28α is to further process the peptides generated by the 26S particle and generate peptides of a specific size for antigen presentation (*8*, *59*). PA28α and PA26 subunits do not share sequence similarities, but both form heptameric ring structures and enhance the peptidase activities of the 20S particles in an ATP-independent manner (*19*, *24*). Importantly, the PA26-activated 20S proteasomes do not degrade substrate proteins (*19*), although the pore size of the *T. brucei* 20S proteasome seems larger than that of the yeast proteasome and resembles the size of the pore of prokaryotic proteasomes (*36*). On the basis of these intriguing findings, it may be argued that machinery that degrades peptides in *T. brucei* is not the Ub−proteasome system but involves other nonidentified ATP-dependent (?) proteases [like in prokaryotes (*35*, *60*)]. According to this hypothesis, PA26 complex would perform a supplementary or regulatory role, analogous to that of PA28α.

On the other hand, the presence of the 26S proteasome in *T. brucei* may have escaped detection because the large and complex 26S particle is unstable and notoriously difficult to isolate. In favor of this idea, the structural and functional properties of the *T. brucei* 20S proteasome resemble those of the yeast and mammalian 20S proteasomes. While prokaryotic 20S particles have only two subunits and display primarily chymotryptic-like activity, the yeast, mammalian, and *T. brucei* 20S proteasomes contain 14 different subunits and display more than one peptidase activity (*36*, *37*). It should also be pointed out that sequences with high homology to 26S components have been reported in the *T. brucei* databank (S4, 098693; S6a, AQ658101; S6b, AQ649013; S7, AQ941695; and S8, AQ637851).[3]

In an attempt to identify *T. cruzi* proteins that are targeted for degradation by the 26S proteasome, we analyzed the fate of cytoskeletal proteins during transformation of trypomastigotes into amastigotes, when the flagellum almost disappears, and the parasite dramatically changes its shape. As shown in Figure 6, there is an increase in the conjugation of ubiquitin to flagellar proteins during transformation, and ubiquitinated products accumulate in the presence of lacta-

cystin. Although the preparation used in these experiments contained predominantly paraflagellar rod proteins (PAR) and tubulin as seen by staining with Coomassie blue, we failed to identify the ubiquitinated proteins. By immunoprecipitations with antibodies against PAR molecules, we did not detect the presence of an associated ubiquitin moiety (not shown). Nevertheless the interpretation of these experiments is problematic because paraflagellar rod proteins are notoriously difficult to solubilize. Further studies are necessary to unravel the participation of Ub−proteasome pathway in the sequence of events that leads to the precisely timed disassembly and disappearance of the complex matrix of paraflagellar rod proteins and axoneme. Some of the questions to be asked are (i) Which signaling pathways are triggered in trypomastigotes when the pH is lowered to 5.0? (ii) Since the flagellar rod is a rigid and highly insoluble lattice-like structure, how are the constituent proteins disassembled and how do they enter the Ub−proteasome system? Do proteasomes and calpains specifically associate with the flagellum and with the rod during transformation? (iii) What are the end products of the destruction of the rod? (iv) Do they find their way into the cytoplasm of the host cells, or are they reutilized by the amastigotes? Some of these questions are relevant to other Trypanosomid parasites of the genera *Trypanosoma* and *Leishmania* that remodel their flagellar structures during development in the insect and/or mammalian hosts.

ACKNOWLEDGMENT

Dr. E. J. Corey and Dr. H. Pleogh generously provided lactacystin and carboxybenzyl-leucyl-leucyl-leucine vinyl sulfone (Z-L3VS).

REFERENCES

1. Andrews, N. W. (1995) *Trends Cell Biol. 5*, 133−137.
2. Ley, V., Robbins, E. S., Nussenzweig, V., and Andrews, N. W. (1990) *J. Exp. Med. 171*, 401−413.
3. Kanbara, H., Uemura, H., Nakazama, S., and Fukama, T. (1990) *Jpn. J. Parasitol. 39*, 226−228.
4. Tomlinson, S., Vandekerckhove, F., Frevert, U., and Nussenzweig, V. (1995) *Parasitology 110*, 547−554.
5. Goldberg, A. L., Akopian, T. N., Kisselev, A. F., Lee, D. H., and Rohrwild, M. (1997) *Biol. Chem. 378*, 131−140.
6. Pagano, M. (1997) *FASEB J. 11*, 1067−1075.
7. Pahl, H. L., and Baeuerle, P. A. (1996) *Curr. Opin. Cell Biol. 8*, 340−347.
8. Groettrup, M., Souza, A., Kuckelkorn, U., and Kloetzelt, P. M. (1996) *Immunol. Today 17*, 429−435.
9. Bonifacino, J. S., and Weissman, A. M. (1998) *Annu. Rev. Cell. Biol. 14*, 19−57.
10. Schubert, U., Antón, L. C., Gibbs, J., Norbury, C. C., Yewdell, J. W., and Bennink, J. R. (2000) *Nature 404*, 770−774.
11. Coux, O., Tanaka, K., and Goldberg, A. L. (1996) *Annu. Rev. Biochem. 65*, 801−847.
12. Ferrell, K., Wilkinson, C. R. M., Dubiel, W., and Gordon, C. (2000) *Trends Biochem. Sci. 25*, 83−88.
13. Lowe, J., Stock, D., Jap, B., Zwicki, P., Baumeister, W., and Huber, R. (1995) *Science 268*, 533−539.
14. Seemüller, E., Lupas, A., Stock, D., Lowe, J., Huber, R., and Baumeister, W. (1995) *Science 268*, 579−582.
15. Voges, D., Zwickl, P., and Baumaeister, W. (1999) *Annu. Rev. Biochem. 68*, 1015−1068.
16. Verma, R., and Deshaies, R. J. (2000) *Cell 101*, 341−344.
17. Glickman, M. H., Rubin, D. M., Fried, V. A., and Finley, D. (1998) *Mol. Cell. Biol. 18*, 3149−3162.
18. Dubiel, W., Pratt, G., Ferrell, K., and Reichesteiner, M. (1992) *J. Biol. Chem. 267*, 22369−22377.
19. Yao, Y., Huang, L., Krutchinsky, A., Wong, M. L., Standing, K. G., Burlingame, A. L., and Wang, C. C. (1999) *J. Biol. Chem. 274*, 33921−33930.
20. Preckel, T., Fung-Leung, W. P., Cai, Z., Vitiello, A., Salter-Cid, L., Winqvist, O., Wolfe, T. G., Von Herrath, M., Angulo, A., Ghazal, P., Lee, J. D., Fourie, A. M., Wu, Y., Pang, J., Ngo, K., Peterson, P. A., Fruh, K., and Yang, Y. (1999) *Science 286*, 2162−2165.
21. Fenteany, G., Standaert, R. F., Lane, W. S., Choi, S., Corey, E. J., and Schreiber, S. L. (1995) *Science 268*, 726−731.
22. Gonzalez, J., Ramalho-Pinto, F. J., Frevert, U., Ghiso, J., Tomlinson, S., Scharfstein, J., Corey, E. J., and Nussenzweig, V. (1996) *J. Exp. Med. 184*, 1909−1918.
23. Mutomba, M. C., To, W. Y., Hyun, W. C., and Wang, C. C. (1997) *Mol. Biochem. Parasitol. 90*, 491−504.
24. To, W. Y., and Wang, C. C. (1997) *FEBS Lett. 404*, 253−262.
25. Saborio, J. L., Hernandez, J. M., Narayanswami, S., Wrightsman, E. P., and Manning, J. (1989) *J. Biol. Chem. 264*, 4071−4075.
26. Eytan, E., Ganoth, D., Armon, T., and Hershko, A. (1989) *Proc. Natl. Acad. Sci. U.S.A. 86*, 7751−7755.
27. Rivett, A. J., Savory, P. J., and Djaballah, H. (1994) *Methods Enzymol. 244*, 330−350.
28. Sogin, M. L. (1991) in *The Phylogenetic Significance of Sequence Diversity and Length Variations in Eukaryotic Small Subunit Ribosomal RNA Coding Regions* (Warren, L., and Koprowski, H., Eds.), pp 175−188, New Perspectives On Evolution, Wiley, New York.
29. Figuereido-Pereira, M. E., Narik, N., and Wilk, S. (1994) *J. Neurochem. 62*, 1989−1994.
30. Cazzulo, J. J. (1992) *Subcell. Biochem. 18*, 235−257.
31. Johnston, N. L., and Cohen, R. E. (1991) *Biochemistry 30*, 7514−7522.
32. Huber, C. M., Saffrich, R., Ansorge, W., and Just, W. W. (1999) *EMBO J. 18*, 5476−5485.
33. Sadigursky, M.; Santos-Buch C. A. (1997) *Recept. Signal Transduct. 7*, 29−43.
34. Finley, D., Tanaka, K., Mann, C., Feldmann, H., Hochstrasser, M., Vierstra, R., Johnston, S., Hampton, R., Haber, J., Mccusker, J., Silver, P., Frontali, L., Thorsness, P., Varshavsky, A., Byers, B., Madura, K., Reed, S. I., Wolf, D., Jentsch, S., Sommer, T., Baumeister, W., Goldberg, A., Fried, V., Rubin, D. M., Glickman, M. H., and Toh-e, A. (1998) *Trends Biochem. Sci. 23*, 245−246.
35. Gottesman, S., Wickner, S., and Maurizi, M. R. (1997) *Genes Dev. 11*, 815−823.
36. Hua, S−b., To, W.-Y., Nguyen, T. T., Wong, M.-L., and Wang, C. C. (1996) *Mol. Biochem. Parasitol. 78*, 33−46.
37. Huang, L., Shen, M., Chernushevich, I., Burlingame, A. L., Wang, C. C., and Robertson, C. D. (1999) *Mol. Biochem. Parasitol. 102*, 211−223.
38. Robertson, C. D. (1999) *Mol. Biochem. Parasitol. 103*, 49−60.
39. Emmerlich, V., Santarius, U., Bakker-Grunwald, T., and Scholze, H. (1999) *Mol. Biochem. Parasitol. 100*, 131−134.
40. Gonzalez, J., Bai, G., Frevert, U., Corey, E. J., and Eichinger, D. (1999) *Eur. J. Biochem. 264*, 897−904.
41. Scholze, H., Frey, S., Cejka, Z., and Bakker-Grunwald, T. (1996) *J. Biol. Chem. 271*, 6212−6216.
42. Rubin, D. M., Glickman, M. H., Larsen, C. N., Dhruvakumar, S., and Finley, D. (1998) *EMBO J. 17*, 4909−4919.
43. Richmond, C., Gorbea, C., and Rechsteiner, M. (1997) *J. Biol. Chem. 272*, 13403−13411.
44. Craiu, A., Gaczynska, M., Akopian, T., Gramm, C. F., Fentany, G., Golberg, A. L., and Rock, K. L. (1997) *J. Biol. Chem. 272*, 13437−13445.
45. Rock, K. L., Gramm, C., Rothstein, L., Clark, K., Stein, R., Dick, L., Hwang, D., and Goldberg, A. L. (1994) *Cell 78*, 761−771.
46. Kirchhoff, L. V., Kim, K. S., Engman, D. M., and Donelson, J. E. (1988) *J. Biol. Chem. 263*, 12698−12704.
47. Swindle, J., Ajioka, J., Eisen, H., Sanwal, B., Jacquemot, C., Browder, Z., and Buck, G. (1988) *EMBO. J. 7*, 1121−1127.

48. Horrocks, P., and Newbold, C. I. (2000) *Mol. Biochem. Parasitol. 105*, 115−125.
49. Olaya, P., and Wasserman, M. (1991) *Biochim. Biophys. Acta. 1096*, 217−221.
50. Bhattacharya, J., Dey, R., and Datta, S. C. (1993) *Mol. Cell. Biochem. 126*, 9−16.
51. Ridgley, E. L., Xiong, Z. H., and Ruben, L. (1999) *Biochem. J. 340*, 33−40.
52. Carafoli, E., and Molinari, M. (1998) *Biochem. Biophys. Res. Commun. 247*, 193−203.
53. Goll, D. E., Thompson, V. F., Taylor, R. G., and Zalewska, T. (1992) *Bioessays 14*, 549−556.
54. Ruiz, R. C., Favoreto, S., Jr., Dorta, M. L., Oshiro, M. E., Ferreira, A. T., Manque, P. M., and Yoshida, N. (1998) *Biochem. J. 330*, 505−5011.
55. Docampo, R., and Moreno, S. N. J. (1996). *Parasitol. Today 12*, 61−65.
56. Lu, H.-G., Zhong, L., de Souza, W., Benchimol, M., Moreno, S., and Docampo, R. (1998) *Mol. Cell. Biol. 18*, 2309−2323.
57. Gantt, S., Myung, J. O., Briones, M. R. S., Li, W. D., Corey, E. J., Omura, S., Nussenzweig, V., and Sinnis, P. (1998) *Antimicrob. Agents. Chemother. 42*, 2731−2738.
58. Mutomba, M. C., and Wang, C. C. (1998) *Mol. Biochem. Parasitol. 93*, 11−22.
59. Bochtler, M., Ditzel, L., Groll, M., Hartmann, C., and Hubert, R. (1999) *Annu. Rev. Biophys. Biomol. Struct. 28*, 295−317.
60. Kim, Y.-I., Burton, R. E., Burton, B. M., Sauer, R. T., and Baker, T. A. (2000) *Mol. Cell 5*, 639−648.

BI001659K